REPORT DOCUMENTATION PAGE

Form Approved
OMB No. 0704-0188

1. REPORT DATE *(DD-MM-YYYY)*	**2. REPORT TYPE**	**3. DATES COVERED** *(From - To)*
26-08-2016	Journal Article	1 Jan 2016 – 31 Jul 2016

4. TITLE AND SUBTITLE

Dual-modulation, dual-wavelength, optical polarimetry system for glucose monitoring

5a. CONTRACT NUMBER

5b. GRANT NUMBER

5c. PROGRAM ELEMENT NUMBER
N/A

6. AUTHOR(S)

Zhen Fang Yu
Casey W. Pirnstill
Gerard L. Cote

5d. PROJECT NUMBER
N/A

5e. TASK NUMBER

5f. WORK UNIT NUMBER

7. PERFORMING ORGANIZATION NAME(S) AND ADDRESS(ES) AND ADDRESS(ES)
Texas A&M University Biomedical Engineering Department
5045 Emerging Technologies Building
3120 TAMU
College Station, TX 77843-3120

8. PERFORMING ORGANIZATION REPORT NUMBER
N/A

9. SPONSORING / MONITORING AGENCY NAME(S) AND ADDRESS(ES)
Air Force Materiel Command
Air Force Research Laboratory
711 Human Performance Wing
Human Effectiveness Directorate
Warfighter Interface Division
Applied Neuroscience Branch
Wright-Patterson AFB OH 45433

10. SPONSOR/MONITOR'S ACRONYM(S)
711 HPW/RHCP

11. SPONSOR/MONITOR'S REPORT NUMBER(S)

12. DISTRIBUTION / AVAILABILITY STATEMENT

DISTRIBUTION STATEMENT A: Approved for public release: distribution unlimited.

13. SUPPLEMENTARY NOTES
88ABW Cleared 04/05/2016; 88ABW-2016-1739. Report contains color. [DOI: 10.1117/1.JBO.21.8.087001]

14. ABSTRACT

A dual modulation optical polarimetry system utilizing both laser intensity and polarization modulation was designed, built, and tested. The system was designed to reduce complexity and enhance the speed in order to facilitate the reduction of motion-induced time-varying birefringence, which is one of the major limitations to the realization of polarimetry for glucose monitoring in the eye. The high-speed less complex technique was tested using in vitro phantom studies with and without motion artifact introduced. The glucose concentration ranged from 0 to 600 mg⁄dl and the glucose measurements demonstrated a standard error of prediction to within 8.1 mg⁄dl without motion and to within 13.9 mg⁄dl with motion. Our feedback control systems took less than 10 ms to reach stabilization, which is adequately fast to eliminate the effect of time-varying birefringence. The results indicate that this new optical polarimetric approach has improved the speed and reduced the complexity, showing the potential for it to be used for noninvasive glucose measurements.

15. SUBJECT TERMS
Optical activity; polarimetry; glucose monitoring; noninvasive; motion artifact.

16. SECURITY CLASSIFICATION OF:			**17. LIMITATION OF ABSTRACT**	**18. NUMBER OF PAGES**	**19a. NAME OF RESPONSIBLE PERSON**
a. REPORT	**b. ABSTRACT**	**c. THIS PAGE**			Casey Pirnstill
Unclassified	Unclassified	Unclassified	SAR	25	**19b. TELEPHONE NUMBER** *(include area code)*

Dual-modulation, dual-wavelength, optical polarimetry system for glucose monitoring

Zhen fang Yu[a,b], Casey W. Pirnstill[b,c], Gerard L. Coté[b,d]

[a]School of Optoelectronic Information, University of Electronic Science and Technology of China, Cheng Du, China, 610054

[b]Texas A&M University, Department of Biomedical Engineering 5045 Emerging Technologies Building 3120 TAMU, College Station, TX 77843-3120

[c]711th Human Performance Wing, Human Effectiveness Directorate, Warfighter Interface Division, Applied Neuroscience Branch, WPAFB, OH 45433

[d]Center for Remote Health Technologies and Systems, Texas A&M University Experiment Station, College Station, TX,77843

Abstract: Using optical polarimetry for probing aqueous humor glucose concentrations has the potential for ascertaining blood glucose noninvasively. One major limiting factor for the realization of polarimetry is time-varying corneal birefringence due to motion artifact. To enhance the speed of the polarimetry system and provide real time closed-loop feedback at two wavelengths that can help overcome the time-varying birefringence, a dual-modulation system was designed, built and tested. This new system utilized laser intensity and polarization modulation to increase the frequency. This configuration also reduced the system complexity by reducing the number of detectors from two to one. In this study, the high speed technique was developed and *in vitro* phantom studies were performed with and without motion. The glucose concentration ranged of 0-600 mg/dl and the glucose measurements demonstrated the sensitivity and accuracy of the system to within 10 mg/dl without motion and within 14 mg/dl with motion. Our feedback control systems took less than 10 ms to reach stabilization, which is adequately fast to eliminate the effect of time-varying birefringence. The results indicate that this new optical polarimetric approach has improved the speed and reduced the complexity, showing the potential for it to be used for non-invasive glucose measurements.

Keywords: optical activity, polarimetry, glucose monitoring, noninvasive, motion artifact.

Address all correspondence to: Gerard L. Coté, Texas A&M University, Department of Biomedical Engineering, Emerging Technologies Building, MS 3120, College Station, TX 77843-3120. Tel: 979-845-4196. Email: gcote@tamu.edu

1. Introduction

Diabetes afflicts an estimated 347 million people worldwide and nearly 29.1 million people in the United States[1–2]. Diabetes, along with its associated complications is ranked as the seventh leading cause of death[1–2]. Intensive management of blood sugars is an effective way to prevent or at least slow the progression of diabetic complications such as heart disease, blindness and kidney disease. To provide this management requires frequent monitoring of glucose levels followed by mitigation via insulin or lifestyle changes[3]. Currently, the most common commercial methods for glucose monitoring are invasive and require a blood sample from the patients' finger or forearm each time a reading is needed. In some cases, patients use continuous glucose monitoring (CGM) approaches, which requires an indwelling probe, typically inserted in the abdomen. Although the CGM approaches provide continues data they require frequent calibration, the probes need to be replaced typically every 3 and 7 days depending on the brand[4]. Both of the finger/forearm stick and CGM approaches can be painful, uncomfortable, and can lead to infection for the end user[5]. Therefore, development of a noninvasive sensor can overcome these problems, greatly enhance the experience for the end user, and potentially facilitate better management of diabetes.

Over the past few decades, many companies and universities have and are attempting to quantify glucose using various noninvasive optical methods, which include, but are not limited to Raman spectroscopy[6–7,] near-infrared spectroscopy[8–9], optical coherence tomography[10–11], photoacoustic spectroscopy[12], fluorescence[13–14]

and optical polarimetry[15–17]. Each of these approaches has their strengths and drawbacks as covered not only in the above articles but in several good review articles on the topic[4,18-21] and so we will not go into detail here on each of them but rather focus on the polarimetric approach.

Optical polarimetry applied to glucose detection relies on optical activity or rather chirality of the glucose molecule, which rotates the polarization plane of a linearly polarized light. The amount of rotation is proportional to specific rotation, the concentration of the optically active compound and the length of the sample. The following equation describes this interaction between an optical active molecule with polarized light, namely,

$$[\alpha]_\lambda = \frac{\alpha}{LC} \qquad (1)$$

in which $[\alpha]_\lambda$ is the specific rotation of the optically active molecule at a given wavelength (λ), α is the observed rotation, C is the sample concentration and L is the sample path length.

Optical polarimetry was first used in the food industry, and a precise polarimeter was proposed by Gillham[22]. In 1982, polarimetry for use in measuring glucose concentration in the aqueous humor of the eye was first proposed by March and Rabinovitch[16]. The aqueous humor of the eye was chosen and shown by this group as a potential sensing site for polarimetric quantification of glucose. The advantages are that the aqueous humor glucose is correlated with blood glucose and it is a clear medium with negligible loss of polarization due to scattering effects. In 1992, a true phase measurement was developed by Coté et. al demonstrating the potential for

millidegree sensitivity in glucose-doped water solution[23], meanwhile, Goetz et.al constructed a polarimetric system with microdegree accuracy[24–25]. In 1997, Cameron reported a polarimetric system with a digital closed-loop control system significantly improving the sensitivity and repeatability of the previous system[26]. Time-varying corneal birefringence due to motion artifacts was discovered as a potential noise source and a dual-wavelength polarimetric approach was proposed by Wan et al.[27] to minimize the effect of this birefringence. The system designed did not allow for real-time feedback and thus was not adequate for *in vivo* studies. Malik[28] constructed a closed-loop dual-wavelength polarimetric system utilizing a real-time feedback controller. This system reduced the contribution of the time-variant corneal birefringence, but the overall response time of this system was roughly 300 ms, which was limited by the Faraday modulator's modulation frequency. This dual-wavelength polarimetry closed-loop approach was sufficiently fast enough to show some success in measuring glucose concentrations in the presence of motion induced birefringence within moving cuvette, *in vitro* with a plastic eye phantom, and *in vivo* in New Zealand White (NZW) rabbits under anesthesia[27–30]. In order to decrease the stabilization time, Grunden et. al.[31] presented a higher speed polarimetric system using a ferrite based Faraday modulator. Using the new ferrite Faraday modulator provided improved system response speed. In this dual-wavelength system, the lasers are powered with a constant DC voltage and the polarization is modulated using a single Faraday rotator which required two detectors for differentiating the two wavelength signals. These systems also suffered from electromagnetic interference

(EMI) and $1/f$ noise. To date, these studies have been performed using an eye coupling device on anesthetized rabbits with minimal motion and, although the results are promising, by enhancing the system speed and reducing the system complexity, as shown here, a more effective and efficient system is anticipated that will provide near real time monitoring needed to overcome the noise from time-varying birefringence expected in further *in vivo* studies.

2. Materials and Methods

2.1 Dual-wavelength, dual-modulation, optical polarimeter

The optical configuration of our experiment is illustrated in Figure 1 and includes a 635 nm laser diode emitting at 7 mW (Power Technology Inc., Little Rock, AR, USA) as well as a green laser diode emitting 22 mW of power at a wavelength of 515 nm (Oxxius S.A. Lannion, France). The lasers were modulated using synchronous sinusoidal signals and linear amplifiers (carrier frequencies: f_{c1}=45kHz, $f_{c2}=82kHz$). The sinusoidal signals were generated from synchronous sine wave generator programmed in LabVIEW 10.0 (National Instruments, Austin, TX, USA) and implemented through a PCI-6713 card (National Instruments, Austin, TX, USA). The modulated beams from both sources were linearly polarized in the horizontal direction employing Glan-Thompson 100,000:1 linear polarizers (P) (Newport, Irvine, California, USA). The individual beams propagated through respective in-house-built Faraday compensators (FC) that serve as rotation compensators in order to achieve closed-loop feedback control. These compensators were made of 1-cm-long terbium-gallium-garnet (TGG) crystals (Deltronic Crystal Inc., Dover, New Jersey,

USA) which were inside bobbins wrapped with electrical magnetically coated coils of wire. TGG crystal was employed since it provided a high Verdet-constant to get the desired optical rotation for the generated field without losing a significant amount of optical signal transmitted through it. The two beams were made coincident by a beam splitter/combiner (BS). The amplitude of each beam was modulated by a ferrite based Faraday modulator (FM) at frequency of $f_m = 8.75kHz$. The coil around the ferrite core was powered with an audio amplifier (Radio Shack, Fort Worth, TX, USA) connected in series with a 0.18 μF capacitor in order to achieve resonance at the modulation frequency. The modulation frequency signal was derived from the same synchronous sine wave generator which was used to power the lasers. Following the ferrite-based Faraday modulator, the light beam proceeded through a rectangular sample cell (Starna Cells Incorporated, Atascadero California, USA) constructed of birefringent material with a path length of 1 cm. Following the sample was a second Glan-Thompson polarizer, known as the analyzer, which was oriented perpendicular to the initial polarizer in the layout. Since the combined light beams at the two wavelengths each had separate carrier modulated frequencies (f_{c1}, f_{c2}), detection could be performed using a single biased photo-diode light detector (Thor Labs, Inc., Newton, NJ, USA), which converted the optical signals into electrical signals. The electrical signals were amplified by a wide-bandwidth transimpedance amplifier (CVI Melles Griot, Albuquerque, NM, USA) and fed into two lock-in amplifiers (Stanford Research Systems, Sunnyvale, CA, USA). The DC output voltages from the lock-in amplifiers served as the inputs to proportional-integral-derivative (PID) controllers

programmed in LabVIEW (10.0, 32 bit, National Instruments, Austin, TX, USA) using a field programmable gate array (FPGA), which provided real-time, closed-loop, feedback. The outputs from the PID controllers were used to drive the respective Faraday compensators via linear driver circuitry. This circuitry provided sufficient current to each Faraday compensator to produce rotations originating from the combination of the glucose and induced birefringence changes with motion artifact.

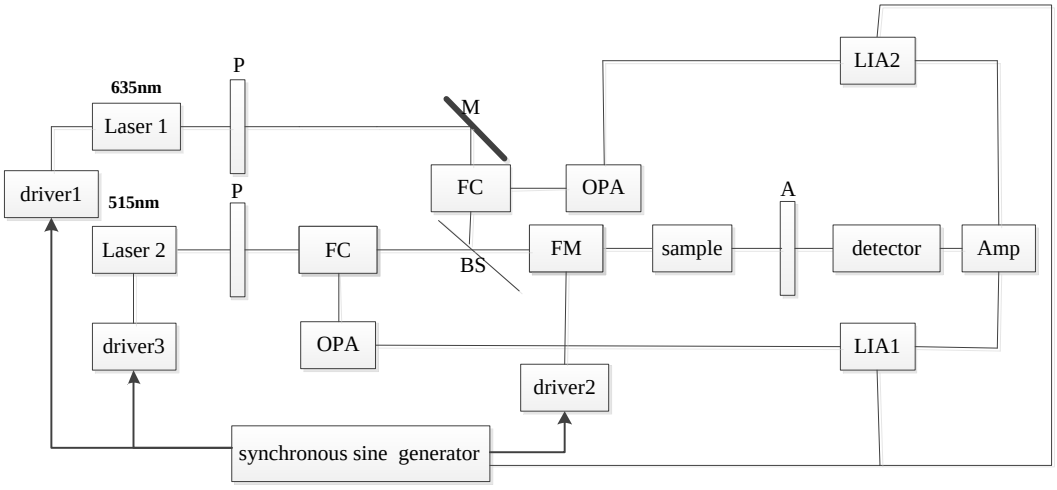

Figure 1: Block diagram of dual-modulation, dual-wavelength, optical polarimetry system

2.2 Mathematical description of the system

Without laser modulation, the intensity detected by the detector for each wavelength in the closed-loop system is derived by Jones vectors and matrices and can be described by the following equation,

$$I \propto E^2 = \left(\varphi^2 + \frac{\theta_m^2}{2} \right) + 2\varphi\theta_m \sin(2\pi f_m)t - \frac{\theta_m}{2}\cos(4\pi f_m)t \qquad (2)$$

where I is the intensity of the detected signal, φ is the rotation due to the optically active sample, θ_m is the modulation depth of the Faraday modulator, f_m is the modulation frequency from the faraday rotator and t is time.

For the dual-modulation, dual-wavelength system, the lasers were modulated by sinusoidal signals at frequencies of f_{c1}=45kHz, $f_{c2}=82kHz$ respectively and were also synchronously modulated by the Faraday rotator at a frequency of $f_m=8.75kHz$. Due to the crossed-polarized nature of the alignment and according matrices for the optical components presented in the block diagram in Fig.1, the detected signal of each wavelength can be represented as:

$$I_i \propto V_{DCi}\left(\varphi_i^2+\frac{\theta_m^2}{2}\right)+\left(\varphi_i^2+\frac{\theta_m^2}{2}\right)V_{ci}sin2\pi f_{ci}t+\varphi_i\theta_m V_{ci}\cos 2\pi(f_{ci}-f_m)t-\varphi_i\theta_m V_{ci}\cos 2\pi(f_{ci}+f_m)t$$
$$-\frac{\theta_m^2 V_{ci}}{4}\sin 2\pi(f_{ci}-2f_m)t-\frac{\theta_m^2 V_{ci}}{4}\sin 2\pi(f_{ci}+2f_m)t+2V_{DCi}\varphi_i\theta_m\sin(2\pi f_m t)+\frac{V_{DCi}\theta_m^2}{2}\cos(4\pi f_m t) \quad (3)$$

where V_{ci} represents the amplitude of the sinusoidal signal at each wavelength, f_{ci} is the carrier frequency of each of the laser modulation signals, and the subscript, *i*, is either 1 or 2, depending on whether it is the first or second laser modulation wavelength. Thus, the major components of the detected signal at each wavelength include f_{c1}, f_{c2} , $2f_m$, $f_{c1}\pm 2f_m$, $f_{c2}\pm 2f_m$ and noise. Equation (3) describes the detected intensity of the light from each wavelength at any instance in time. As can be seen, depending on the concentration of sample and the wavelength of light used, a different sideband frequency component $f_{c1}\pm f_m$, $f_{c2}\pm f_m$ was observed which had a proportional increase with the increase in the rotation, φ_i. Two lock-in amplifiers were used to lock into the detected signals at the frequency of interest, namely, $f_{c1}+f_m$ and $f_{c2}-f_m$ to extract the information carried by each wavelength, which in turn was processed to obtain the concentration of the glucose in the sample. Since the lock-in amplifiers locked in to the sum of the modulation frequency and one of the carrier frequencies, phase sensitive detection was used. In order to measure the amplitude

of the signals at a specified reference frequency, the frequency and phase stability had to be maintained to prevent signal drift, and hence a synchronous sinusoidal signal generator programmed in LabVIEW 10.0 and implemented through PCI-6713 was used to generate the carrier signals, modulation signal, and reference signals.

2.3 Theoretical description for overcoming motion artifact

Mathematically, as noted above, the operation of each of the single wavelengths is based on Eq. 3. From Eq. 3, it is evident that with any optically active sample the signal has DC terms and, at each wavelength, has major frequency components at $f_{c1}, f_{c2}, 2f_m, f_{c1} \pm 2f_m, f_{c2} \pm 2f_m$ and without an optically active sample there are no components at $f_{c1} \pm f_m, f_{c2} \pm f_m$, because the rotation, φ_i, due to glucose is zero. So when an optically active element such as glucose is present the rotation, φ_i, will cause the intensity of detected signal to vary at the frequencies of $f_{c1} \pm f_m, f_{c2} \pm f_m$ and the signals at these frequencies proportionally increase with the increase in the rotation, φ_i, depending on the concentration of sample and the wavelength (i=1 or i=2) of light used. So locking into one of sideband frequency signals provides glucose concentration information carried by each wavelength.

In a closed loop system, if there is minimal birefringence (i.e. not enough to make the polarization become circular) and the birefringence of the sensing site did not change, the glucose concentration could be extracted from the feedback voltage to the Faraday compensators from either wavelength signal, since each compensates for the rotation in polarization due to glucose. In this case, φ_{gi}, (rotation at wavelength i due

to glucose) is equal to φ_{fi} (rotation at wavelength *i* fed back to the Faraday compensator), although the rotation is different for each wavelength and follows Drudes law. However, when motion artifact is introduced into the system, φ_i becomes a function of birefringence, glucose, and the feedback of the Faraday for a given wavelength: $\varphi_i = \varphi_{gi} + \varphi_{bi} - \varphi_{fi}$, where, φ_{bi}, is the rotation induced by the birefringence from each wavelength, but the relationship between φ_{b1} and φ_{b2} are fixed as long as the wavelengths are known because birefringence is a function of both the wavelength and birefringence $|n_e - n_o|$ for a fixed path length through sample. Birefringence for an individual wavelength can be expressed as $\varphi_{b,i}(t) = \frac{2\pi}{\lambda_i}|n_e - n_o|L(t)$, which is constant with wavelength at a given position, a behavior attributed to the form birefringence of the cornea[32-34].

For the case of minimal, non-varying birefringence (without motion), the relation between the feedback voltage and glucose concentration is linear, a linear regression is then used to predicted glucose concentrations, and a predicted concentration model for individual wavelength takes the form: $\text{Glucose}_{pred} = slope*[V(t)] + b$, where $V(t)$ is the compensation voltage signal applied to the Faraday compensator for each wavelength used to null the detected signal via a closed-loop PID controller, Glucose_{pred} is the predicted concentration of the sample, $slope$ and b are the slope and intercept of calibration line determined by the regression model respectively for each wavelength. As stated, since the rotation due to glucose varies with wavelength following Drudes equation, the values for each are not identical. For the dual wavelength system, a multiple regression model was used to determine the glucose

concentration and the model had the form: $\text{Glucose}_{pred} = slope_1 * [V_1(t)] + slope_2 * [V_2(t)] + b$, where $V_1(t)$ and $V_2(t)$ are the feedback voltage obtained to nullify the system for the corresponding dual-wavelength system and $slope_1, slope_2$ and b are the calibration coefficients calculated by multiple linear regression (MLR) model. This MLR model has been shown to minimize the effect of time-varying birefringence caused by motion using the dual-wavelength polarimetric system due to the difference in the signal from glucose rotation with wavelength (Drudes equation) and the relative common mode noise in each wavelength from time-varying birefringence.

3. Results and discussion

A series of experiments was performed on the new dual-modulation, dual-wavelength, system in order to assess its time response and determine its sensitivity *in vitro* across the physiological range of glucose both without and with the presence of time-varying birefringence.

A. Speed determination of the system

As mentioned above, a previous attempt to minimize the effect of time-varying corneal birefringence in the eye that used a dual-wavelength system was only modulated at 1.09 kHz and required 100 ms time constant setting on the lock-in amplifiers, resulting in around 300 ms response time to stabilize the system[28]. With our new system the time response was measured by visualizing the response speed of the feedback voltage produced by the control system. One widely used measure of the speed of response is the 10% to 90% rise time or the amount of time the system takes

to go from 10% to 90% of the steady-state. For the response speed studies, 300 μs was the lock-in amplifier time constant that was used. In Figures 2 and 3, the feedback voltages at as a function of time for the single wavelength systems (515 nm and 632 nm, respectively) are depicted. The plots indicate that the PID control system can reach stability in less than 10 ms which is approximately 30 times faster compared with the real-time, dual-wavelength, approach presented by Malik et al.[28]. This shows that the laser intensity modulation combined with Faraday modulation and an adaptive PID controller can improve the response speed of the system.

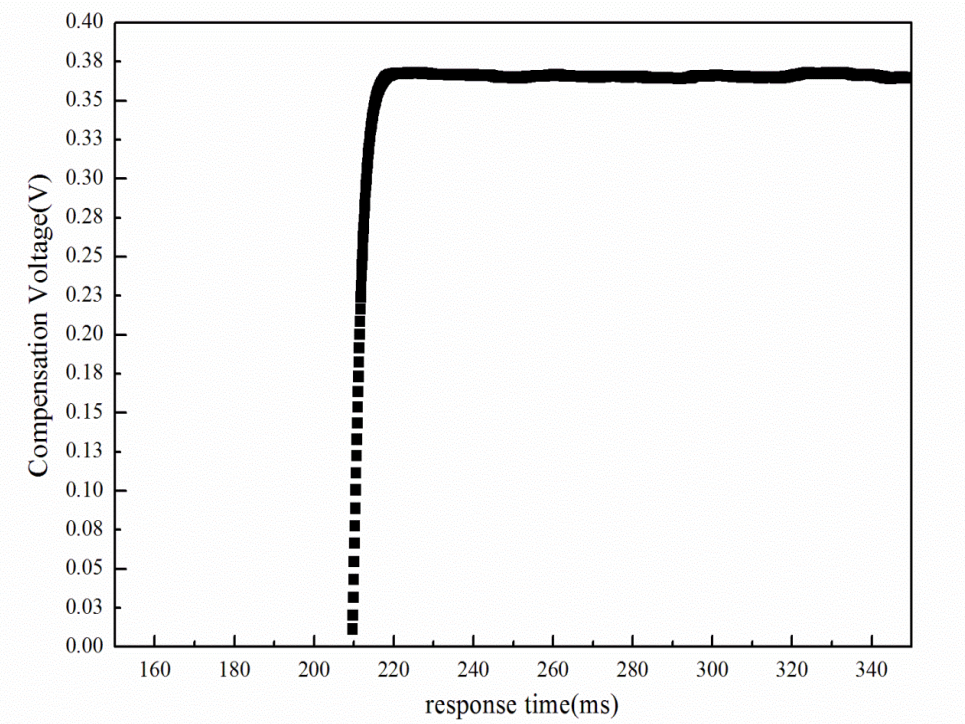

Figure 2: Stabilization of 515 nm PID control system without motion

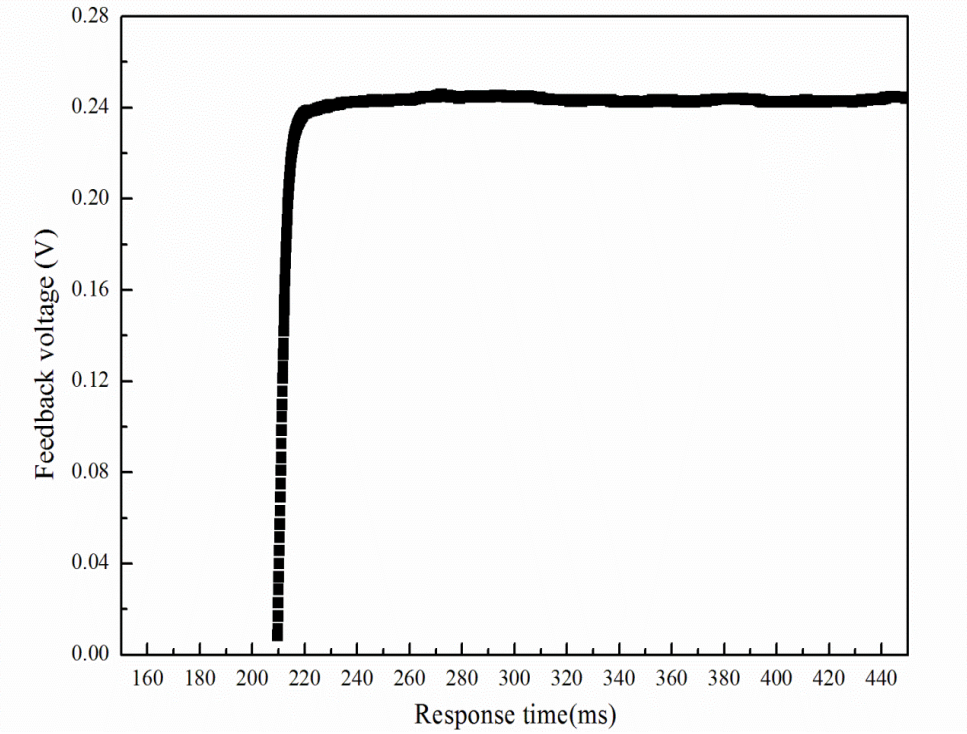

Figure 3: Stabilization of 632 nm PID control system without motion

B. System Performance without Motion

Although it has been shown in the previous section that the new system can provide enhancement in speed, the performance in terms of sensitivity to glucose measurements over the same range as shown previously but requiring less time needs to be determined. The performance of the system was first tested and evaluated for glucose doped water solutions in the motionless system. In particular, a 1 cm rectangular quartz cuvette that allowed for sample to be easily pipetted into was mounted in a fixed holder. The experiments were performed for individual glucose samples between the concentration range of 0-600 mg/dl. All samples were created from a 1000 mg/dl stock glucose solution with a pH of 7.2. The stock solution was made by dissolving 1.0 g of D-glucose (EM Science) into 100 ml de-ionized water and was mixed with a magnetic stirrer for 8 hours in order to completely dissolve the

solute. The stock solution was left undisturbed for at least 3 hours to allow for mutarotation. The sample cell was in a fixed position for each sample in the motionless system.

The motionless system was calibrated and then the glucose concentrations were calculated using a simple linear regression model of the data acquired without motion[35]. In each experiment, three runs of data were recorded for the two wavelengths, 635 nm and 515 nm, respectively. The predicted versus actual glucose concentrations were plotted for the single wavelength system as shown in Figures 4 and 5 respectively. One can see that a high degree of linearity exists given the correlation coefficients for the green (515 nm) light are $r_1 = 0.9990$, $r_2 = 0.9993$, $r_3 = 0.9993$ and for the red (635 nm) light are $r_1 = 0.9985$, $r_2 = 0.9993$, $r_3 = 0.9990$ respectively. Further, the average standard error of prediction (SEP) for the validation of the glucose doped water was 6.48 mg/dl for the green light and 7.18 mg/dl for the red light. The feedback voltages for both wavelengths were applied in a multiple linear regression model and Figure 6 shows the estimated glucose concentration as a function of the actual glucose concentration when both wavelengths are taken into account. Without motion you would expect very light improvement and indeed one can see that a high degree of linearity still exists for all three cases since each correlation coefficient exceeds 0.9996 and the SEP is slightly less than using each wavelength alone ranging from 4.23-5.63 mg/dl, with no outliers present in any of three data runs.

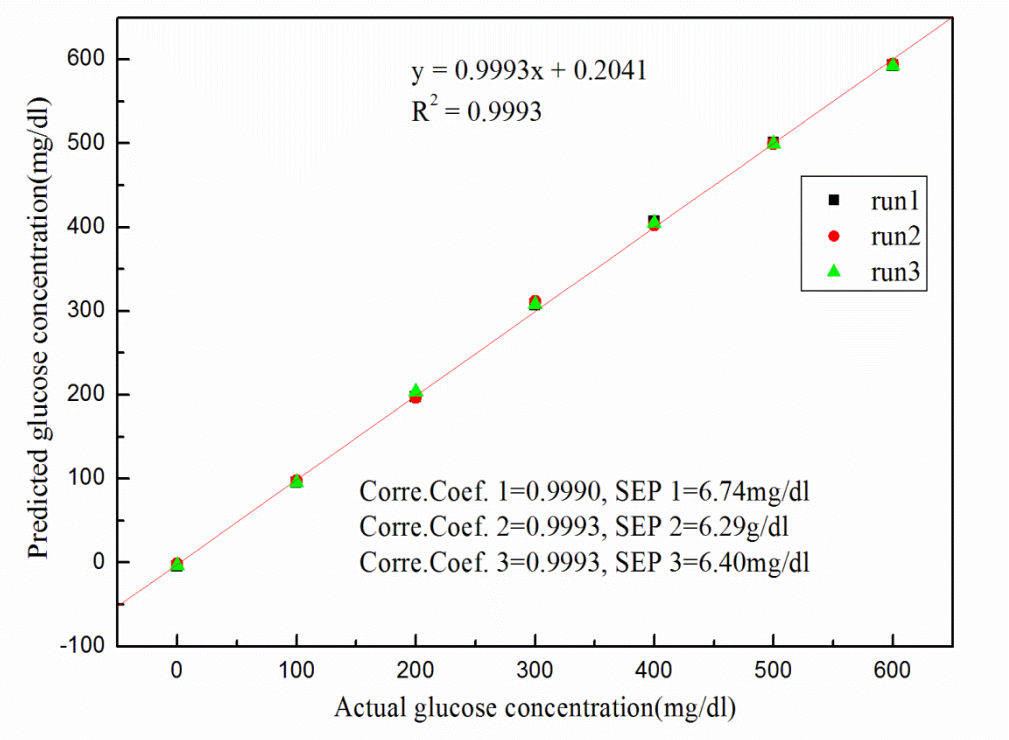

Figure 4: Predicted glucose concentration as a function of actual glucose concentration for the 515 nm laser without motion using a single linear regression model

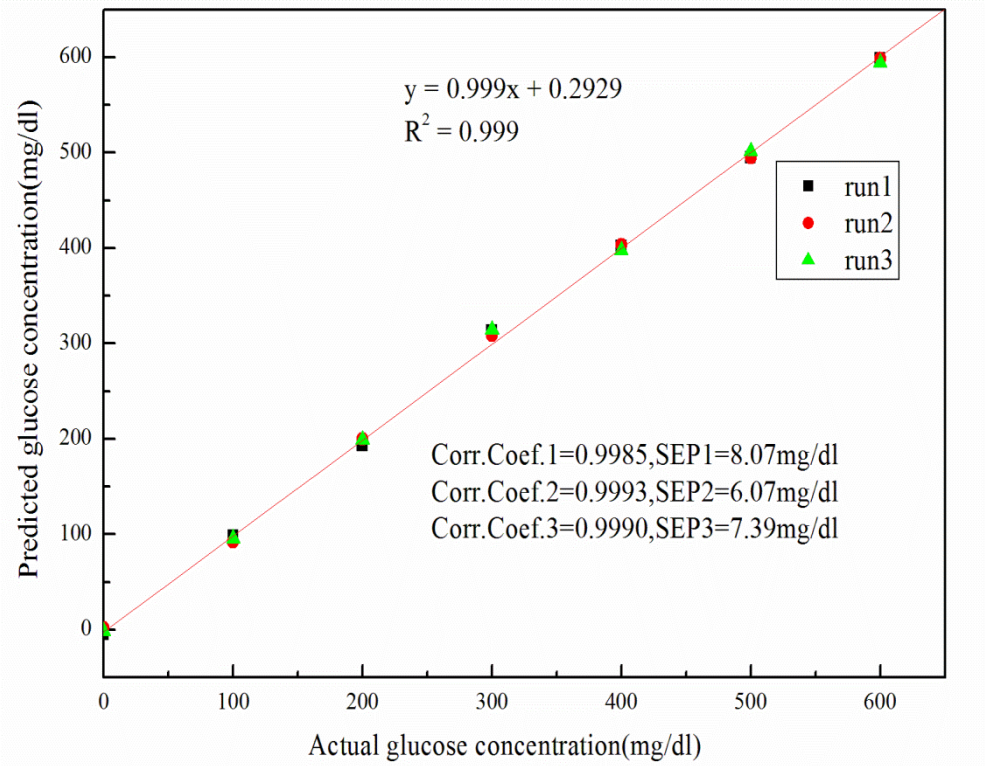

Figure 5: Predicted glucose concentration as a function of actual glucose concentration for the 632 nm laser wavelength without motion using a single linear regression model

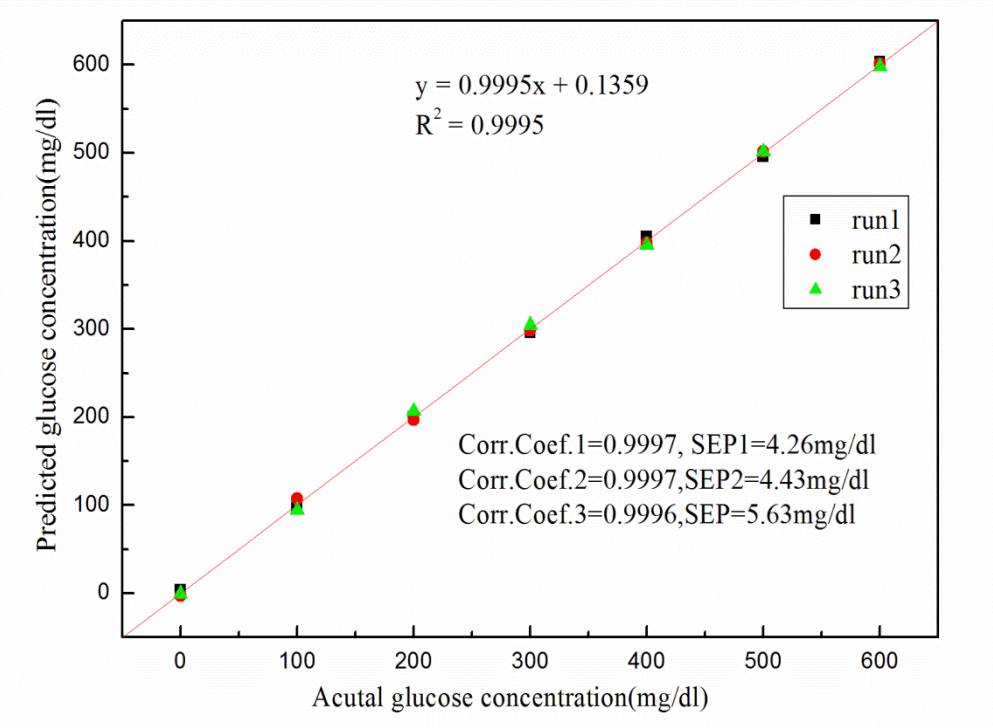

Figure 6: Predicted glucose concentration as a function of actual glucose concentration for the combined 632 nm and 515 nm laser wavelengths without motion using a multiple linear regression model

C. System performance with motion from time-varying birefringence

The experiments were conducted to test the performance of the system for glucose solution in the sample cell while introducing motion into the system. For these experiments, the test cell was mounted on a programmable translation stage (Thorlabs, Newtown, NJ, USA) and the stage was controlled by a T-Cube DC Servo Motor Controller (Thorlabs, Newtown, NJ, USA) and allowed to move up and down to simulate the birefringence changes of the cornea due to motion artifact. The speed and distance of the translation of the motor stage was controlled by a visual basic program.

The system with motion was calibrated and the glucose concentrations were extracted using a linear regression model. This was done for glucose concentrations from 0-600mg/dl.

In order to compare the results of the single wavelength closed-loop and dual wavelength closed-loop system, actual versus predicted glucose concentration for glucose-doped water coupled with a varying birefringence signal using the single wavelength closed-loop system for each wavelength (515nm and 635 nm) is plotted in Figures 7 and 8 . As shown in Figures 7 and 8, the glucose concentrations cannot be predicted very well using a single closed-loop system, since the change in the birefringence of the sample masks the optical rotation due to glucose in the sample. Thus, the single wavelength model has an SEP over 100 mg/dl in the presence of birefringence changes due to motion.

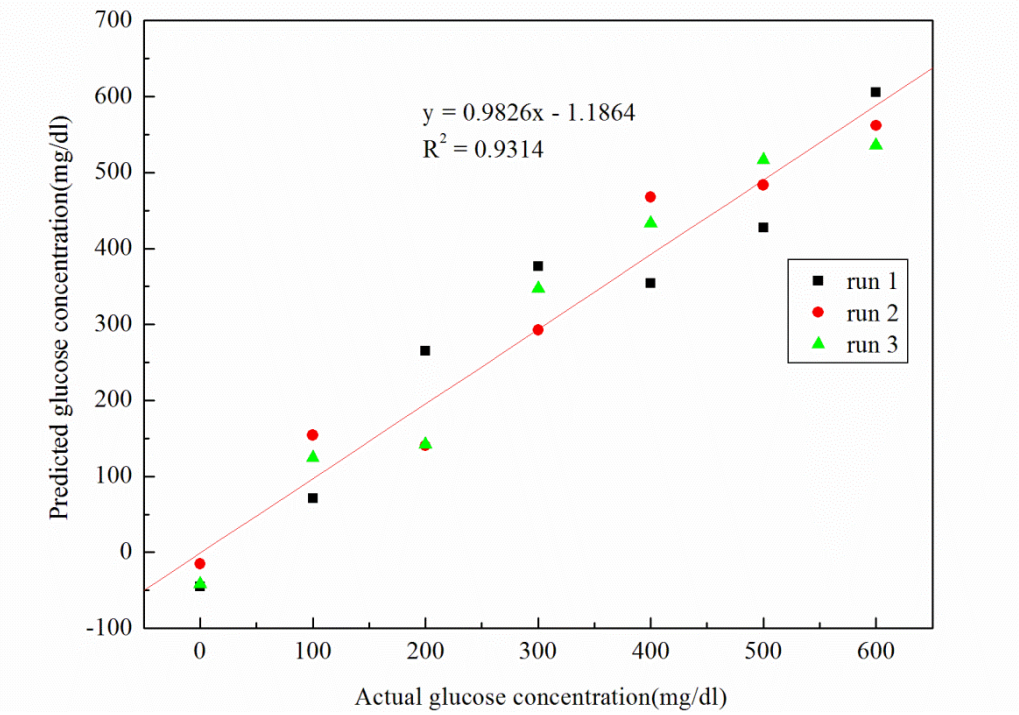

Figure 7: Actual versus predicted glucose concentration for glucose-doped water in the presence of time varying birefringence due to motion using a single wavelength closed-loop system for 515nm

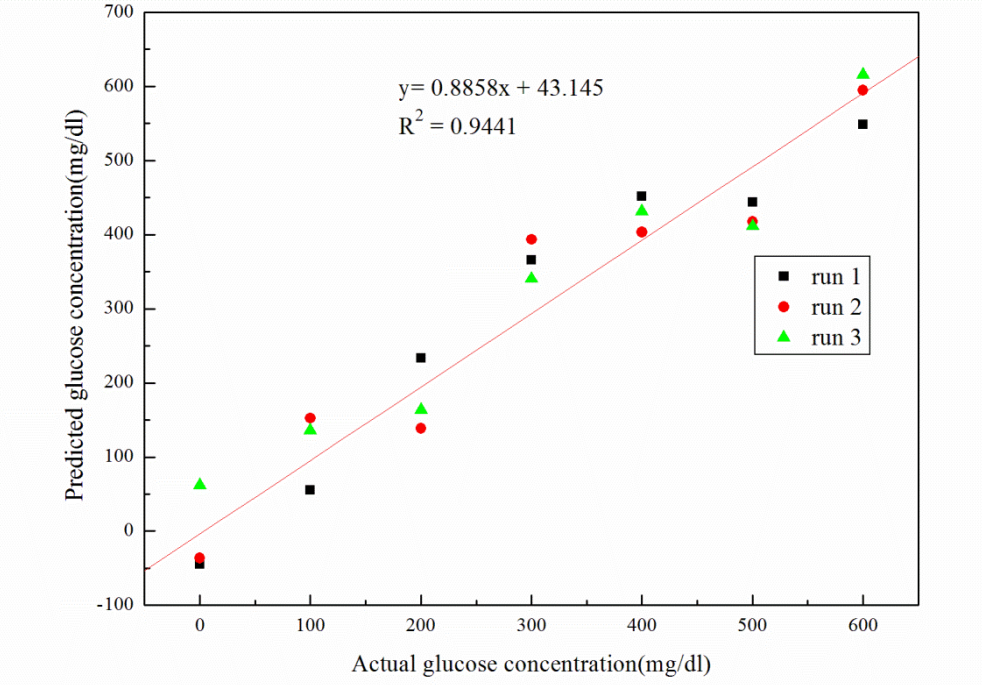

Figure 8: Actual versus predicted glucose concentration for glucose-doped water in the presence of time varying birefringence due to motion using a single wavelength closed-loop system for 635nm

The predicted concentrations results for the dual wavelength experiments using MLR calibration are illustrated in Figure 9. The predicted calibration results when both wavelengths are used to compensate for the correlated noise due to motion showed a high degree of linearity with all correlation coefficients exceeding 0.9972 and the standard errors of prediction of 13.0 mg/dl, 13.7 mg/dl and 13.9 mg/dl as depicted in Figure 9. No outliers were present in any of the data sets. Although the SEP was greater than the motionless system, it was still as good as the previous slower system and, although a very simple sample, was still within the range needed for noninvasive glucose monitoring.

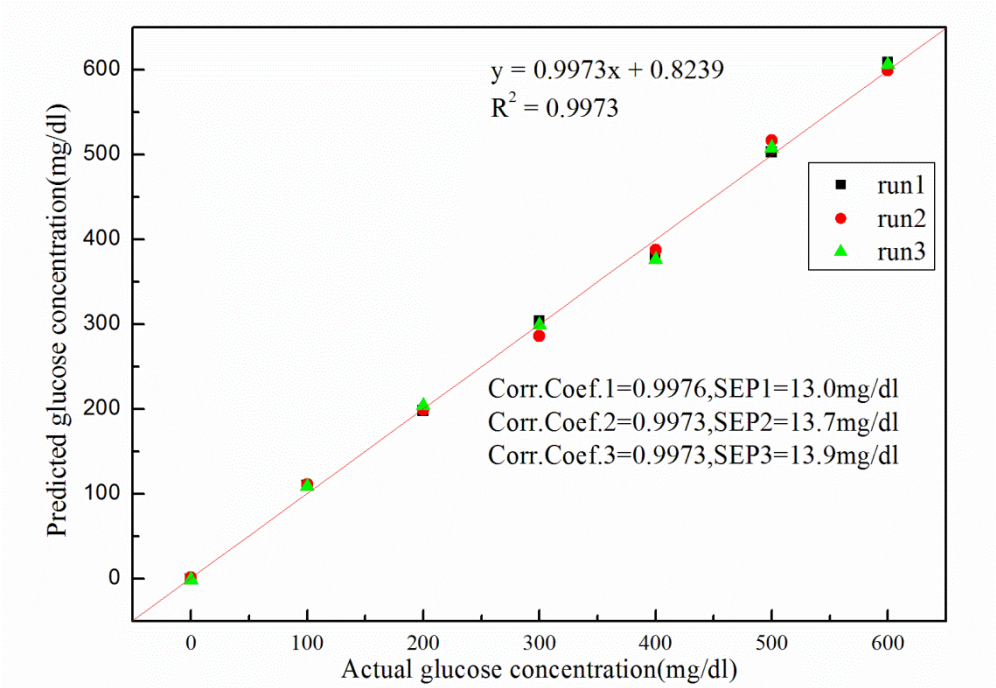

Figure 9: Predicted glucose concentration as a function of actual glucose concentration with motion due to time-varying birefringence calculated using an MLR regression model for 632 nm and 515 nm wavelengths

4. Conclusions

In summary, a dual-modulation, dual-wavelength, near real-time closed-loop polarimeter system for glucose monitoring was presented that utilized the combination of laser modulation and Faraday polarization modulation for each wavelength simultaneously. This approach was shown to increase the speed over previous systems by 30 times with a stability of less than 10 ms. Further, the system complexity was reduced by removing one detector from the previous system configuration. Lastly, the *in vitro* glucose measurement results with and without motion demonstrate the sensitivity of the system to be within 9 mg/dl and 14 mg/dl respectively, indicating equivalent sensitivity to the previous slower systems with less complexity showing the potential for its utility as a noninvasive glucose monitoring system.

Acknowledgments

The authors wish to acknowledge the financial support from the program of China Scholarships Council (CSC). The authors would like to thank Danial Grundan, former M.S. student in the Optical Biosensing Laboratory at Texas A&M, and Qiu Qi, professor of School of Photoelectronic Information at the University of Electronic Science and Technology of China, for their assistance and helpful technical discussions. As per SPIE guidelines, the authors acknowledge the SPIE Photonics West proceedings number 9715-29, in which part of this work was presented in San Francisco, CA on Feb. 16, 2016.

References

1. Global status report on noncommunicable diseases 2010. Geneva, World Health Organization (2011).
2. Centers for Disease Control and Prevention. National Diabetes Statistics Report: Estimates of Diabetes and Its Burden in the United States, Atlanta, GA: U.S. Department of Health and Human Services (2014).
3. T. D. Control and Complications Trial Research Group, "The effect of intensive treatment of diabetes on the development and progression of long-term complications in insulin-dependent diabetes mellitus," *N. Engl. J. Med.* **329**, 977-986 (1993).
4. S. K. Vashist, "Continuous glucose monitoring systems: A Review," Diagnostics **3**, 385-412 (2013).
5. T. Koschinsky, and L. Heinemann, "Sensors for glucose monitoring: technical and clinical aspects," *Diabetes Metab. Res. Rev.* **17**, 113-123 (2001).

6. A. M. Enejder, T.G. Scecina, J. Oh et al., "Raman spectroscopy for noninvasive glucose measurements," *J. Biomed. Opt.* **10**(3), 031114 (2005).

7. M.J. Scholtes-Timmerman, S. Bijlsma, M. J. Fokkert et al., "Raman spectroscopy as a promising tool for noninvasive point-of-care glucose monitoring," *J Diabetes Sci Technol*. **8**(5), 974-979 (2014).

8. J. Yadav, A. Rani, V. Singh et al., "Prospects and limitations of non-invasive blood glucose monitoring using near-infrared spectroscopy," *Biomedical Signal Processing and Control* **18**, 214-227(2015).

9. M. Goodarzi, S. Sharma, H. Ramon, W. Saeys, "Multivariate calibration of NIR spectroscopic sensors for continuous glucose monitoring," *TrAC Trends in Analytical Chemistry* **67**, 147-158 (2015).

10. K.V. Larin, M. Motamedi, T.V. Ashitkov, R.O. Esenaliev, "Specificity of noninvasive blood glucose sensing using optical coherence tomography technique: a pilot study," *Physics in Medicine and Biology* **48**(10), 1371 (2003).

11. K. V. Larin, M. S. Eledrisi, M. Motamedi, "Noninvasive blood glucose monitoring with optical coherence tomography," *Diabetes Care* **25**(12), 2263-7 (2002).

12. M.A. Pleitez , T. Lieblein, A. Bauer, O. Hertzberg, H. von Lilienfeld-Toal, W. Mäntele, "In vivo noninvasive monitoring of glucose concentration in human epidermis by mid-infrared pulsed photoacoustic spectroscopy," *Anal.Chem.* **85**(2), 1013–1020 (2013).

13. J. C. Pickup, F. Hussain, N. D. Evans, O. J. Rolinski et al., "Fluorescence based glucose sensors," *Biosensors and Bioelectronics* **20**(12), 2555-2565 (2005).

14. J. C. Pickup, F. Hussain, N. D. Evans, N. Sachedina, "In vivo glucose monitoring: the

clinical reality and the promise," *Biosensors and Bioelectronics* **20**(10), 1897-1902 (2005).

15. R. Marbach, T. Koschinsky, F. A. Gries, and H. M. Heise, "Noninvasive blood glucose assay by Near-Infrared diffuse reflectance spectroscopy of the human inner lip," *Applied Spectroscopy* **47**(7), 875-881 (1993).
16. B. Rabinovitch, W.F. March, and R. L. Adams, "Noninvasive glucose monitoring of the aqueous humor of the eye: part I. measurement of very small optical rotation," *Diabetes Care* **5**(3), 254-258 (1982).
17. W.F. March, B. Rabinovitch, and R.L. Adams, "Noninvasive glucose monitoring of the aqueous humor of the eye: part II. Animal studies and the scleral lens," *Diabetes Care* **5**(3), 259-265 (1982).
18. A. Tura, A. Maran, G. Pacini, "Non-invasive glucose monitoring: Assessment of technologies and devices according to quantitative criteria," *Diabetes Research and Clinical Practice* **77**(1), 16-40 (2007).
19. C. E. Ferrante do Amaral, B. Wolf, "Current development in non-invasive glucose monitoring," *Medical Engineering & Physics* **30**(5), 541-549 (2008).
20. S. K. Vashistr, "Non-invasive glucose monitoring technology in diabetes management: A review," *Analytica Chimica Acta* **750**, 16–27 (2012).
21. J. L. Smith, "The pursuit of noninvasive glucose: 'Hunting the deceitful turkey,' " Fourth Edition: Revised and Expanded, parts copyright by John L. Smith 2015 (http://www.mendosa.com/The%20Pursuit%20of%20Noninvsive%20Glucose,%20Fourth%20Edition.pdf).

22. E. J. Gillham, "Photoelectric polarimeter using the Faraday Effect," *Nature* **178**, 1412-1413 (1956).

23. G. L. Coté, M. D. Fox, and R. B. Northrop, "Noninvasive optical polarimetric glucose sensing using a true phase measurement technique," *IEEE TRANSACTIONS ON BIOMEDICAL ENGINEERING* **39**(7), 752-756 (1992)

24. M. J. Goetz, Jr., "Microdegree polarimetry for glucose detection," M.S. thesis, Univ. Connecticut, Storrs, CT (1992).

25. M. J. Goetz, Jr., M. D. Fox, and R. B. Northrop, "Microdegree polarimetry using a diode laser for glucose detection," in *Proc. 18th IEEE Annual Northeast Bioengineering Conf.* pp. 97–98, IEEE, NewYork (1992).

26. B. D. Cameron and G. L. Coté, "Noninvasive glucose sensing utilizing a digital closed-loop polarimetric approach," *IEEE Trans.Biomed.Eng*. **44**, 1221-1227 (1997).

27. Q. Wan, G. L. Coté, and J. B. Dixon, "Dual-wavelength polarimetry for monitoring glucose in the presence of varying birefringence," *J.Biomed. Opt.* **10**(2), 024029 (2005).

28. B. H. Malik, and G. L. Coté, "Real-time, closed-loop dual-wavelength optical polarimetry for glucose monitoring," *J.Biomed. Opt*. **15**(1), 017002 (2010).

29. B. H. Malik, C. W. Pirnstill, and G. L. Coté, "Dual wavelength polarimetric glucose sensing in the presence of birefringence and motion artifact using anterior chamber of the eye phantoms," *J Biomed Opt.* **18**(1), 017007-1-9 (2013).

30. C. W. Pirnstill, B. H. Malik et al., "In vivo glucose monitoring using dual-wavelength polarimetry to overcome corneal birefringence in the presence of motion," Diabetes Technology & Therapeutics **14**(9), 819-27 (2012).

31. D. T. Grunden, C. W. Pirnstill, and G. L. Coté, "High-speed dual-wavelength optical polarimetry for glucose sensing," *SPIE* **8951**, 895111-1-6 (2014).

32. R. Knighton, X.-R. Huang, and L. A. Cavuoto, "Corneal birefringence mapped by scanning laser polarimetry," *Opt.Express* **16**(18), 13738–13751 (2008).

33. R. Kingston, "Spectral dependence of corneal birefringence at visible wavelengths," *Invest. Ophthalmol. Vis. Sci.* **43**, 152 (2002).

34. K. Irsch et al., "Modeling and minimizing interference from corneal birefringence in retinal birefringence scanning for foveal fixation detection," *Biomed. Opt. Express* **2**(7), 1955–1968 (2011).

35. C. W. Pirnstill, D. Grunden, and G. L. Coté, "Polarimetric glucose sensing in vitro: a high frequency approach," Proc. *SPIE* **8591**, 859101-859101-7 (2013).